Segmental Versican Expression in the Trabecular Meshwork and Involvement in Outflow Facility

Kate E. Keller, John M. Bradley, Janice A. Vranka, and Ted S. Acott

Purpose. Versican is a large proteoglycan with numerous chondroitin sulfate (CS) glycosaminoglycan (GAG) side chains attached. To assess versican's potential contributions to aqueous humor outflow resistance, its segmental distribution in the trabecular meshwork (TM) and the effect on outflow facility of silencing the versican gene were evaluated.

Methods. Fluorescent quantum dots (Qdots) were perfused to label outflow pathways of anterior segments. Immunofluorescence with confocal microscopy and quantitative RT-PCR were used to determine versican protein and mRNA distribution relative to Qdot-labeled regions. Lentiviral delivery of shRNA-silencing cassettes to TM cells in perfused anterior segment cultures was used to evaluate the involvement of versican and CS GAG chains in outflow facility.

Results. Qdot uptake by TM cells showed considerable segmental variability in both human and porcine outflow pathways. Regional levels of Qdot labeling were inversely related to versican protein and mRNA levels; versican levels were relatively high in sparsely Qdot-labeled regions and low in densely labeled regions. Versican silencing decreased outflow facility in human and increased facility in porcine anterior segments. However, RNAi silencing of ChGn, an enzyme unique to CS GAG biosynthesis, increased outflow facility in both species. The fibrillar pattern of versican immunostaining in the TM juxtacanalicular region was disrupted after versican silencing in perfusion culture.

Conclusions. Versican appears to be a central component of the outflow resistance, where it may organize GAGs and other ECM components to facilitate and control open flow channels in the TM. However, the exact molecular organization of this resistance appears to differ between human and porcine eyes. (*Invest Ophthalmol Vis Sci.* 2011;52:5049–5057) DOI: 10.1167/iovs.10-6948

Intraocular pressure (IOP) is primarily controlled by the flow resistance in the aqueous humor outflow pathway.[1,2] Much of this resistance resides within the trabecular meshwork (TM) putatively within 7 to 14 μm of the inner wall of Schlemm's canal in a region known as the juxtacanalicular (JCT) or cribriform region.[1–4] Since the 1950s, involvement of extracellular matrix (ECM) in outflow resistance has commonly been evoked.[1,2,5–10] There is also considerable evidence of a direct contribution to the resistance by some cell populations within this region.[1,3] More recently, synergistic interaction between the JCT and Schlemm's inner wall endothelial cells has been suggested.[1–3,11] However, most of the resistance is still thought to reside within the actual ECM of the JCT.[1–3,11] The most likely extracellular source is the highly charged glycosaminoglycan (GAG) chains.[2,6,12–14] Although perfusion of GAG-degrading enzymes reduces the outflow resistance in numerous species, in humans and primates, this effect has been controversial.[15,16] However, perfusion of inhibitors of GAG biosynthesis or sulfation and with enzymes that degrade ECM proteins reduces outflow resistance in both porcine and human eyes.[17–21]

The identity of the specific GAGs, proteoglycans, or other ECM components that comprise outflow resistance remains unclear.[2] Both conceptually and based on several observations, versican, with supportive contributions from its attached chondroitin sulfate (CS) GAG chains and hyaluronan (HA) interactions, seems a likely contributor.[2,17,22,23] Versican is a large aggregating CS proteoglycan.[2,24] In other tissues, it is involved in a wide array of cellular functions including cell proliferation, migration, and adhesion and acts directly and indirectly via its many binding partners. Unique N- and C-terminal binding domains are separated by two large central domains: α- and βGAG. Alternative mRNA splicing produces four different protein isoforms: V0 contains both α- and βGAG domains, V1 has only βGAG, V2 has only αGAG, and V3 has neither α- nor βGAG domains.[2,24] Up to 23 CS GAG side chains can be attached to these two central domains. These CS chains appear to extend away from the core protein in all directions, thus minimizing electrostatic interactions and filling large hydrodynamic volumes. Conceptually, this design is ideal to regulate movement of aqueous humor through the TM.[25] In addition, versican is essential for assembling HA in the ECM[26] and is important for tissue hydration, as it forms large complexes with HA.[27]

Mechanical stretching or distortion appears to be the mechanism by which TM cells sense elevated IOP and trigger IOP homeostatic responses.[2,17,20,21,28] TM cells respond to mechanical stretching by increasing ECM turnover and decreasing total versican mRNA levels.[2,17,29] We recently found that perfusion of human or porcine anterior segments with ADAMTS4 (a disintegrin and metalloproteinase with thrombospondin motifs 4), which specifically cleaves versican, increases outflow facility.[18] In addition, modified alternative mRNA splicing of versican in response to mechanical stretching shifts isoform distribution to favor transcripts with less GAG side chain attachment sites per molecule.[29] Conversely, TGFβ, which decreases outflow facility, increases versican levels and shifts isoform distributions to favor transcripts with more GAG side chain attachment sites per molecule.[30–33] TNFα and IL-1α, both of which increase outflow facility, also produce changes in versican mRNA level and isoform distribution similar to

From the Casey Eye Institute, Oregon Health and Science University, Portland, Oregon.

Supported by National Institute of Health Grants EY003279, EY008247, and EY010572 (TSA); a Shaffer Award for Innovative Research from the Glaucoma Research Foundation, San Francisco, CA (KEK); and by an unrestricted grant to the Casey Eye Institute from Research to Prevent Blindness, New York, NY.

Submitted for publication November 24, 2010; revised March 29 and April 28, 2011; accepted April 28, 2011.

Disclosure: **K. Keller**, None; **J. Bradley**, None; **J. Vranka**, None; **T. Acott**, None.

Corresponding author: Ted S. Acott, Casey Eye Institute, Oregon Health and Science University, 3181 SW Sam Jackson Park Road, Portland, OR, 97239; acott@ohsu.edu.

those associated with mechanical stretch.[2] Thus, a homeostatic response to elevated pressure may involve versican turnover by ADAMST4, reduction in the amount of versican synthesized as replacement ECM, and modulation of alternative splicing to generate isoforms with fewer CS GAG chain attachment sites.

Several studies have shown that outflow is segmental, rather than uniform, around the circumference of the TM.[34–39] Flow appears higher in areas of the TM near collector channels, suggesting an anatomic contribution to flow segmentation.[35] However, ECM composition may also vary in areas of high or low outflow, either affecting or possibly reflecting relative flow rates. To further evaluate the hypothesis that versican is important to outflow resistance and IOP homeostasis, we used fluorescent quantum dots (Qdots), derivatized to facilitate cellular uptake, to label areas of putative high and low fluid flow in perfused human and porcine anterior segments. Versican mRNA abundance relative to Qdot distribution was assessed by quantitative RT-PCR, and versican protein distribution was analyzed by immunofluorescence and confocal microscopy. RNAi silencing was used to knockdown versican gene expression and also the first unique step in CS GAG biosynthesis to assess outflow effects in anterior segment perfusion culture.

METHODS

Qdot Nanoparticle Labeling of Anterior Segments in Perfusion Culture

For perfusion culture, human and porcine eyes were prepared as described previously and perfused at constant pressure (8.8 mm Hg) to generate an average flow rate of 1 to 7 μL/min for humans and 2 to 8 μL for porcine eyes.[18,19,21,40] Human donor eye pairs were acquired from Lions Eye Bank of Oregon (Portland, OR). Human donor tissue protocols were approved by the Oregon Health and Science University Institutional Review Board and were conducted in accordance with the tenets of the Declaration of Helsinki. Porcine or human anterior segment organ cultures were treated during the final 1 to 2 hours of perfusion experiments with 10 nM fluorescent Qdot nanoparticles (Qtracker 655; Invitrogen, Carlsbad, CA) via direct injection of 200 μL of solution into the inflow line of the flow chamber. These 10- to 20-nm particles are derivatized with a variant of the HIV-TAT peptide, which facilitates cellular uptake and retention. In preliminary studies, we verified that these Qdots were effectively internalized by TM cells, stable to prolonged light exposure, and relatively nontoxic to cultured TM cells. A deep red plasma membrane cellular stain (2.5 μg/mL; CellMask; Invitrogen) was also used to label TM cell membranes for the final 15 minutes of perfusion. After exposure to Qdots or cell membrane stain, anterior segments were removed from the perfusion chambers and the TM analyzed by standard fluorescence microscopy at low magnification and looking en face from the anterior chamber toward Schlemm's canal. Tissues were immediately separated into regions of dense and sparse Qdot-labeling, which appeared to be a direct indicator of outflow such that regions of intense relative fluorescence likely represent sites of high segmental outflow (see Fig. 2). Once isolated, tissue wedges were fixed in 4% paraformaldehyde for immunofluorescence and confocal microscopy analysis, or TMs were removed for RNA extraction.

Two methods were used to process tissues for confocal microscopy: (1) anterior segments were embedded in paraffin and 5-μm serial radial sections were cut approximately perpendicular to Schlemm's canal at the pathology/histology core facility of the Knight Cancer Institute (Oregon Health and Science University, Portland, OR). Qdot fluorescence was generally lost during deparaffinization. Some sections were stained with hematoxylin and eosin (H&E). (2) Frontal sections were cut with a double-edged razor blade perpendicular to the ocular surface, resulting in a section tangential to the corneoscleral limbus that bisects Schlemm's canal.[35,37,41] These sections were placed onto glass microscope slides and imaged by confocal microscopy. Immunofluorescence and confocal microscopy were performed as described previously, with a mouse monoclonal versican antibody (Developmental Studies Hybridoma bank, University of Iowa, Iowa City, IA or Kamiya Biomedical Co., Seattle, WA), a rabbit polyclonal SPARC antibody (Millipore, Temecula, CA), and a rabbit polyclonal CD44 antibody (Sigma-Aldrich, St. Louis, MO).[18,19,42]

RNA Isolation and Quantitative RT-PCR

After Qdot labeling, the TM was dissected from regions of intense, moderate, and sparse labeling from six different anterior segments perfused at physiological pressure for 24 hours. Total RNA was isolated from each region of individual eyes (TRIzol reagent, amplified using the MessageAmp II RNA amplification kit; Ambion, Austin, TX) and subjected to quantitative RT-PCR, as described elsewhere.[18,29] Relative fluorescence units (RFUs) from each region of the six TMs were then averaged and normalized for glyceraldehyde 3-phosphate dehydrogenase (GAPDH) levels. Significance was determined by Student's *t*-test.

Design and Construction of shRNA Silencing Vectors

A vector-based approach was used to express short, hairpin (sh)RNA molecules in TM cells. shRNAs were designed using an online RNAi designer (BLOCK-iT; Invitrogen). Sequences were selected to target the G1 domain of human or porcine versican, which would silence all known mRNA isoforms. An shRNA control was designed to a region approximately 4000 bp upstream of the versican promoter region. This control shRNA did not target any other known human or porcine gene when blasted against the NCBI database. An shRNA was also designed to silence *N*-acetylgalactosaminyltransferase-1 (ChGn), the first unique enzyme in CS chain biosynthesis.[43–45]

Complementary 21-nucleotide shRNA sets were annealed to generate double-stranded (ds) DNA oligonucleotides and cloned into the pENTR/U6 vector using T4 ligase (Invitrogen). The resulting silencing cassette contained a human U6 promoter, the shRNA ds oligonucleotides, and an RNA polymerase III terminator, all the elements required for RNA polymerase III-controlled expression of the silencing shRNA. Correct sequences were confirmed by DNA sequencing. The shRNA cassettes were transferred into the pLenti6/BLOCK-iT-DEST vector by recombination with a clonase enzyme (Gateway LR Clonase II; Invitrogen). This vector contains modified HIV-1 5′ and 3′ long-terminal repeats and an HIV-1 psi sequence for viral packaging, but the VSV-G gene from vesicular stomatitis virus is used in place of the HIV-1 envelope glycoprotein. The pLenti6 silencing vector was transformed into *E. coli* (strain OneShot Stbl3) and purified (Endo-free Plasmid Maxiprep kit; Qiagen, Valencia, CA).

Generation of Versican shRNA Lentivirus

Replication incompetent lentivirus was generated in the 293FT cell line (Invitrogen). The 293FT cells were maintained in Dulbecco's modified Eagle's medium (DMEM) containing 10% fetal calf serum (FCS), 4 mM glutamine, 1 mM minimum essential medium (MEM) sodium pyruvate, 0.1 mM MEM nonessential amino acids, 1% penicillin-streptomycin, and 500 μg/mL geneticin (Invitrogen). The pLenti expression plasmid (3 μg) containing the silencing cassette was co-transfected with 9 μg packaging mix (ViraPower; Invitrogen) into 293FT cells (Lipofectamine 2000; Invitrogen). The transfection reagent-DNA complexes were incubated overnight with the 293FT cells and then replaced with DMEM containing the above supplements without geneticin. Lentiviral-containing supernatants were harvested 72 hours after transfection and centrifuged at 3000 rpm for 10 minutes to pellet cell debris. Viral supernatants were then aliquotted and stored at −80°C until use.

Viral titers were determined and effectiveness of shRNA silencing was assessed by adding various dilutions of lentivirus (ranging from 10^{-2}–10^{-6}) in DMEM+10% FCS or a mock infection to TM cells in culture with 1:1000 dilution of polybrene (Sigma-Aldrich). The virus was replaced by complete medium the following day, and the selection

agent blasticidin (1 μg/mL) was added to the culture 48 hours after infection. After 5 days, adherent cells were washed three times in phosphate-buffered saline (PBS) and stained with 1% crystal violet for 10 minutes. Cells were washed three times in PBS, and the number of stained plaques was counted for each lentiviral dilution. Titers were determined in this manner for each silencing lentivirus in both human and porcine TM cells.

To verify gene knockdown, cultured TM cells were infected with various dilutions of lentivirus (as above), and media were replaced the following day. After 48 hours to allow silencing, total RNA was isolated by using a cells-to-cDNA lysis buffer (Ambion). Quantitative RT-PCR was then performed using versican or ChGn primers. Results were expressed as the ratio of change relative to mock-infected TM cells. To ensure that versican protein was reduced, immunofluorescence was performed on TM cells infected with 10^6 plaque formation units (pfu) of versican-silencing lentivirus. After infection, the cells were grown for a further 72 hours and then immunostained with the primary versican monoclonal antibody and Alexa Fluor 488–conjugated secondary antibody. Images were obtained by confocal microscopy.

Lentiviral Infection of Perfused Anterior Segments

Anterior segments from human and porcine eyes were perfused in culture until the flow rates stabilized. Lentivirus (10^8 pfu) was applied to the perfusion chambers by media exchange (indicated by time point 0), and outflow facility was measured for a further 7 days. The amount of lentivirus used was based on previous studies of lentiviral infection of human and feline TM.[46,47] Outflow rates before treatments were used to normalize for plotting treatment effects. The number of eyes used for each treatment is noted in each figure legend. An unpaired Student's *t*-test was used to determine significance.

Results

Versican Immunostaining in the TM

The distribution of versican in the TM was investigated by immunofluorescence and confocal microscopy (Fig. 1). Versican immunostaining was found throughout the TM beams, in the juxtacanalicular (JCT) region, and at the inner wall (IW) and outer wall (OW) of Schlemm's canal (Fig. 1B). A higher magnification view of a frontal section showed strong versican immunostaining in the JCT region of the TM (Fig. 1C). Versican stains in a striking fibrillar pattern, which is aligned in pillars that are approximately perpendicular to Schlemm's canal. In this image, the versican immunostaining seems to predominate in the deepest regions of the JCT, in the area closest to Schlemm's IW. However, versican staining intensity was somewhat variable in tissue sections originating from different quadrants of the eye. Since prior studies have suggested that outflow appears to be segmental, we further explored the differences in versican immunostaining.

Segmental Flow and Versican Levels

To identify segmental regions of putative high or low outflow, we added Qdots to the perfusate for 1 hour at the end of the perfusion experiments. Both human and porcine anterior segments exhibited considerable segmental variation in Qdot labeling density, which we assume is a direct indicator of outflow. The differences between densely and sparsely labeled areas were often as much as 20-fold (Fig. 2A). Only modest Qdot labeling of corneal endothelial or scleral cells was observed. Even in densely labeled areas, the IW of Schlemm's canal was labeled only moderately, and there was very little OW cell labeling (Fig. 2B). Some labeling of cells lining the collector channels and deeper vasculature could be detected. As a comparison, the red cellular membrane stain (CellMask; Invitrogen) was also used to label areas of outflow. The dye stains cell plasma membranes without the need for active internalization by the cell, hence providing an alternative outflow labeling mechanism. This stain exhibited segmental staining similar to the distribution of Qdots when anterior segments were perfused for the final 15 minutes of the experiment (Figs. 2C, 2D). A longer perfusion time (30 minutes) resulted in more uniform labeling of the TM.

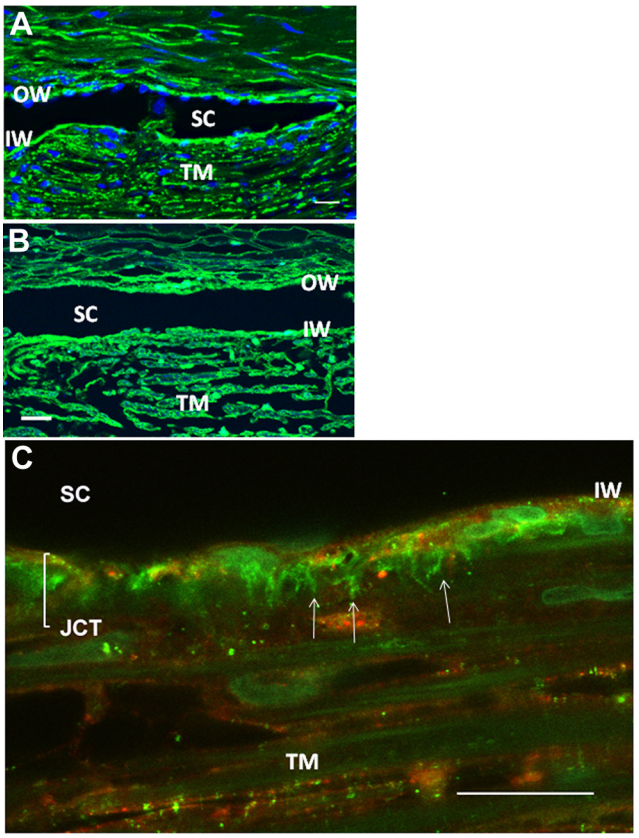

Figure 1. Versican immunostaining in the TM. (**A**, **B**) In paraffin-embedded, radial sections of TM, versican stained the outer TM beams, and the IW and OW of Schlemm's canal (SC). (**C**) Versican immunostaining (*green*) in frontal sections at high magnification shows some fibrillar matrix staining that is aligned in pillars (*arrows*) that are approximately perpendicular to SC and some that is cell associated. SPARC immunostaining (*red*) is primarily cell associated in the JCT. Scale bars, 20 μm.

When versican immunostaining levels were compared to Qdot segmental distributions, an inverse correlation was observed (Fig. 3). Densely labeled areas had relatively low versican immunostaining; sparsely labeled areas had relatively abundant versican immunostaining. The images depicted were from different regions of paraffin-embedded radial sections of one eye (Figs. 3C, 3D) and from frontal sections of paraformaldehyde-fixed TM from a different eye (Figs. 3E, 3F) and were obtained using identical acquisition settings on the confocal microscope. In frontal sections (Figs. 3E, 3F), the pillar pattern of versican immunostaining predominated in the JCT region of densely Qdot-labeled TM, whereas a more uniform distribution of versican was observed throughout the TM of sparsely Qdot-labeled sections.

Versican mRNA Expression and Alternative Splicing

Total RNA was isolated from densely, moderately, and sparsely labeled areas based on Qdot densities, and mRNA levels of

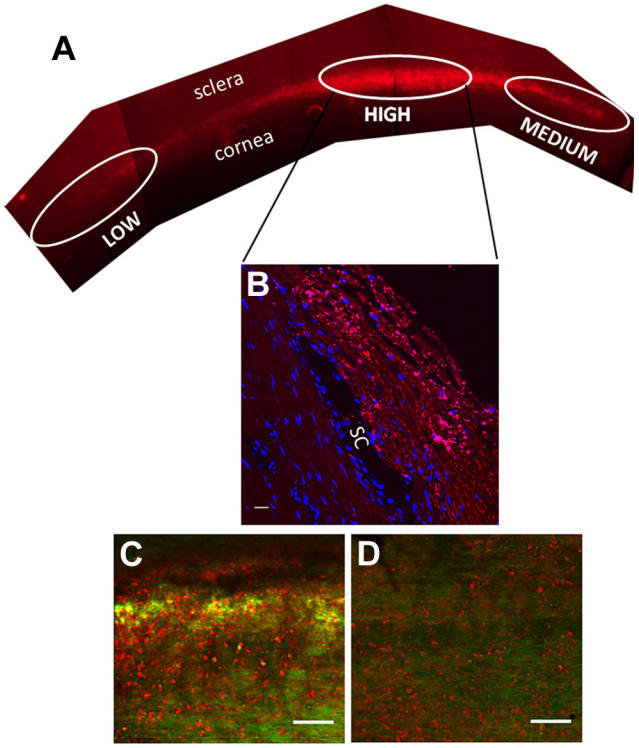

FIGURE 2. Qdot labeling of human anterior segments. (**A**) Human anterior segment viewed en face from the perspective of the anterior chamber showing the distribution of Qdots (*red*) in approximately one quadrant of a human eye. Presumably, the intensity of Qdot labeling is a direct indicator of outflow, such that regions of dense, moderate, and sparse labeling correspond to regions of high, medium, and low outflow through the TM. (**B**) Radial section through a high-labeled region of a human eye showing the distribution of Qdots in the TM (*red*). DAPI was used to stain nuclei (*blue*). SC, Schlemm's canal. (**C**) Comparison of Qdot labeling (*green*) and cell membrane stain (*red*) viewed en face in a high (**C**) and low (**D**) Qdot-labeled area. Scale bar; (**B**) 20 μm; (**C**, **D**) 60 μm.

versican and ADAMTS4 were determined by qRT-PCR (Fig. 4). Versican mRNA levels showed a strong reciprocal relationship to Qdot label density, similar to the protein data, whereas ADAMTS4 mRNA levels were not significantly different between high- and low-density areas.

When the relative distribution of the versican V1 and V2 mRNA alternative splice forms was analyzed using qRT-PCR (Fig. 5), the relative proportion of both isoforms in the densely labeled regions was higher than in the sparsely labeled regions. The V3 variant is absent or present at very low levels in TM cells,[29,33] and so it was not included in this analysis. The V1 and V2 isoform RFU data were normalized for GAPDH mRNA levels and then divided by the regional total versican mRNA level.

Versican Silencing and Outflow Facility

To further evaluate involvement of versican in outflow facility, RNAi was used to selectively reduce versican levels. Various dilutions of lentivirus containing versican shRNA were used to infect porcine and human TM cells in culture, and versican mRNA levels were assessed by qRT-PCR (Fig. 6A). At 10^6 pfu, versican mRNA levels were reduced by approximately 70% after 48 hours when compared with mock-infected TM cells. Versican immunofluorescence was then compared for porcine and human TM cells that had been mock infected (Figs. 6B, 6E), infected with 10^6 pfu control shRNA (Figs. 6C, 6F), or infected with versican shRNA (Figs. 6D, 6G) lentivirus. Both mock-infected and control virus-infected cells showed fibrillar versican immunostaining at 72 hours after infection. This fibrillar staining was dramatically reduced in versican-silenced TM cells.

The control shRNA and versican shRNA lentivirus were then used to perfuse porcine and human anterior segment cultures, and the effects on outflow facility were monitored (Fig. 7). Porcine anterior segments responded to versican silencing with an approximately 2.5-fold increase in outflow rates by 145 hours (Fig. 7A). Conversely, versican-silencing lentivirus reduced outflow in human anterior segments by approximately 50% over a similar time frame (Fig. 7B). Control lentivirus did not significantly change outflow in porcine or human anterior segments. Quantitative RT-PCR using mRNA isolated from two pairs of eyes; one anterior segment of each pair was infected with versican-silencing lentivirus and one was infected with control shRNA lentivirus. The results showed that versican transcripts were reduced by 82% and 61% after approximately 150 hours in perfusion culture when compared with control lentivirus-infected contralateral anterior segments.

Microscopic analysis of human postinfection TM tissue sections stained with hematoxylin and eosin (H&E) showed minimal overall structural differences in the outer TM beams between treatments (Fig. 8). However, closer inspection of the JCT region revealed a disorganized structure in versican-silenced TMs (Fig. 8D). The apparent increase in hematoxylin staining in the JCT of versican-silenced eyes was diminished by pretreating the sections with hyaluronidase. Immunostaining showed that the versican pillar pattern of staining was lost in the JCT region in versican-silenced human TM (Fig. 8F). Instead, a more disorganized punctate pattern was observed.

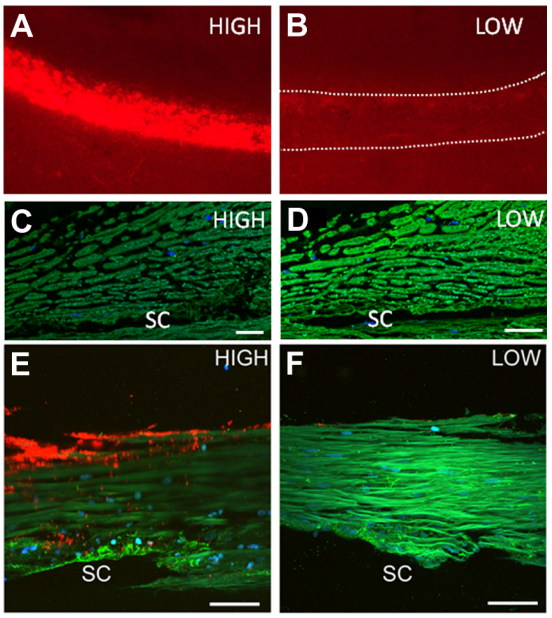

FIGURE 3. Versican immunostaining (*green*) of human anterior segments in areas of dense (**A**, **C**, **E**) and sparse (**B**, **D**, **F**) Qdot labeling (*red*). Versican immunostaining (*green*) in paraffin-embedded radial sections was more abundant in areas of sparse Qdot labeling in the TM (**C**, **D**). Versican immunostaining of frontal sections also shows the inverse relationship between Qdot labeling and versican abundance (**E**, **F**). (**C**, **D**; **E**, **F**) Images shown in were obtained with identical image-acquisition settings on the confocal microscope. DAPI was used to stain nuclei (*blue*). SC, Schlemm's canal. Scale bars: (**C**, **D**) 20 μm; (**E**, **F**) 30 μm.

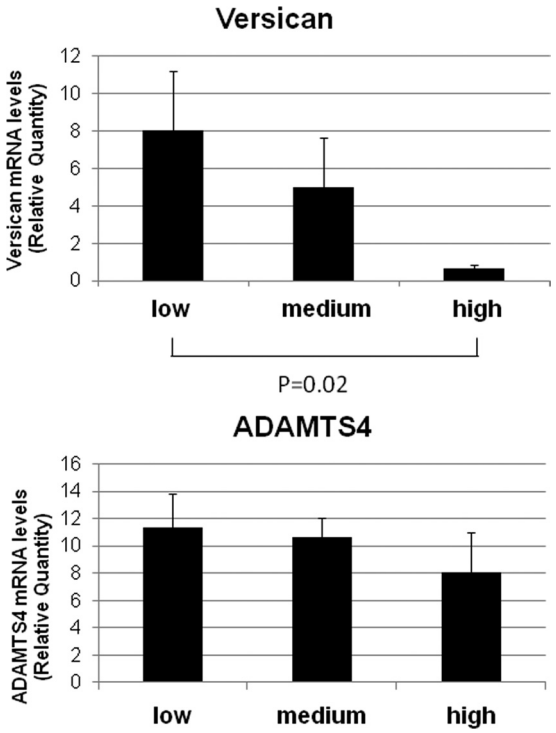

FIGURE 4. Versican and ADAMTS4 mRNA levels in densely and sparsely Qdot-labeled regions. Versican mRNA levels inversely correlated with Qdot labeling patterns; there was high versican mRNA levels in regions of sparse labeling and low levels in densely labeled regions. ADAMTS4, an enzyme that cleaves versican, showed no significant regional distribution. Data were normalized for *GAPDH*. Error bars represent the SEM, where $n = 6$, $P = 0.02$ for versican between high- and low-flow areas.

Silencing CS GAG Chain Biosynthesis and Outflow Facility

To investigate the involvement of CS GAG chains in outflow facility, we silenced *N*-acetylgalactosaminyltransferase-1 (ChGn), the enzyme that catalyzes the first unique step in CS GAG chain biosynthesis.[43,44,48,49] When TM cells in culture were incubated with various dilutions of ChGn shRNA lentivirus and ChGn mRNA levels were assessed, strong mRNA level reductions were achieved in both species at 10^6 pfu (Fig. 9A). Perfusion of anterior segments with ChGn shRNA lentivirus produced an approximately 1.8-fold increase in porcine outflow facility at 120 hours (Fig. 9B) and an approximately 1.4-fold increase in human outflow facility at 140 hours (Fig. 9C). Control lentivirus did not produce any significant change in outflow facility, as shown in Figure 7.

DISCUSSION

Although segmental aqueous humor outflow has long been recognized, the details of this phenomenon are not well understood. In our study, both porcine and normal human TM exhibited distinct segmental distributions with regions of relatively dense, intermediate, and sparse Qdot labeling. Previous methods of evaluating segmental outflow have relied primarily on adsorption of ocular pigment, cationic ferritin, microspheres or labeled dextran beads to charged surfaces, presumably primarily ECM components, within the outflow pathway.[34–37,39,50,51] (Hann CR, et al. *IOVS* 2007;48:ARVO E-Abstract 2053; Overby DR, et al. *IOVS* 2010;51:ARVO E-Abstract 1221). The overall segmental distribution patterns of perfused Qdots, which reflect active cellular uptake, appear to be similar to that in the charged ECM adsorption studies. Moreover, addition of a cell membrane stain, which stains the cell membranes without the need for macropinocytotic uptake into the cell, showed a similar segmental pattern of staining. Collectively, these studies support the argument that the segmental differences observed reflect outflow patterns rather than regional differences in adsorption or uptake. An anatomic relationship between intensely dextran-labeled areas and collector channel distribution has been observed.[35] Although we did not specifically evaluate this relationship, most of the regions labeled with Qdots and viewed en face were much larger and would encompass at least two to five separate collector channels. Therefore, the Qdot segmental labeling patterns seen in this study apparently reflected factors beyond the anatomic distribution of collector channels. The very high degree of segmentation shown in all these studies suggests that regional analyses will be necessary to correlate specific outflow pathway properties with outflow facility.

Versican levels generally showed an inverse segmental relationship to Qdot labeling in the TM. This suggests, but does not prove, a causal relationship in which high versican levels could provide higher resistance to outflow. Regional distributions of versican have also been found in mitral valves, where low versican expression was found in areas of tensile stress, while high versican expression was found in areas subject to compressive forces.[52] The results of perfusion with cytokines (TGFβ2, TNFα, and IL-1α) and the effects of physical manipulations (mechanical stretch, pressure increases, or both) show similar reciprocal relationships between outflow and versican levels or alternative mRNA splicing.[29,53,54] However, these modulation studies reflect overall TM versican levels, and it remains to be established how these are related to flow segmentation.

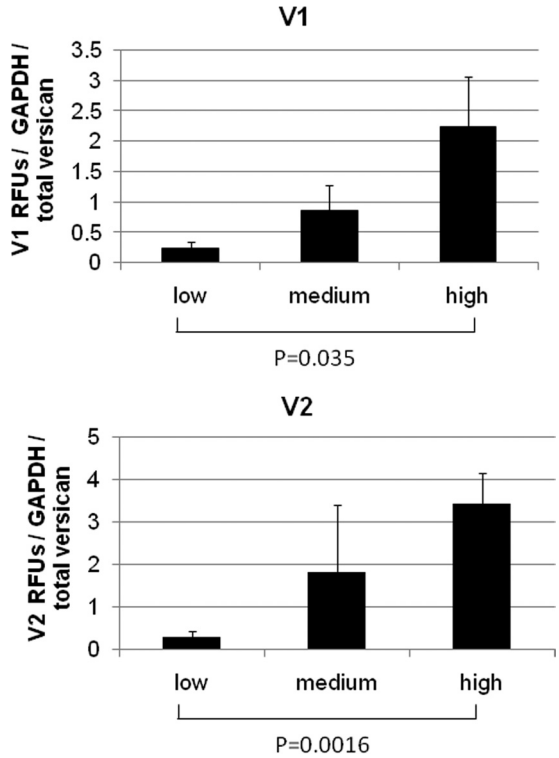

FIGURE 5. Versican V1 and V2 isoforms levels in intensely and weakly labeled regions. Relative fluorescent units (RFUs) were normalized for GAPDH and variations in total versican mRNA levels. Error bars, SEM; $n = 6$. For V1, $P = 0.035$; for V2, $P = 0.0016$.

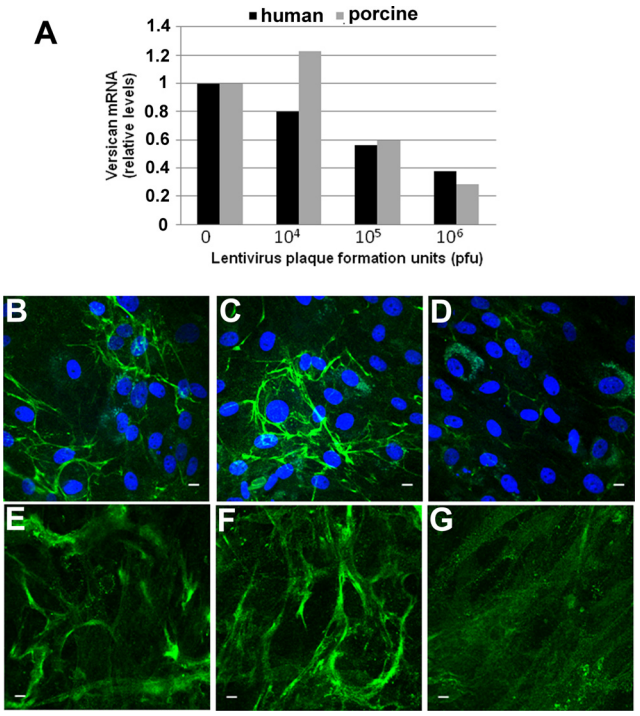

FIGURE 6. Lentiviral shRNA silencing of versican in TM cells. (**A**) The indicated dilutions of versican shRNA lentivirus were added to porcine and human TM cells in culture, and versican mRNA was assessed by qRT-PCR 48 hours later. Values represent the ratio relative to mock-infected TM cells. (**B–G**) Immunofluorescence of porcine (**B–D**) and human (**E–G**) TM cells in culture using a versican monoclonal antibody for (**B**, **E**) mock-infected cells, (**C**, **F**) control lentivirus-infected cells, and (**D**, **G**) versican shRNA lentivirus-infected cells. Immunofluorescence was performed 72 hours after infection. DAPI was used to stain nuclei (*blue*). Scale bars, 10 μm.

In human eyes, reducing versican levels by RNAi led to a loss of pillar-like staining in the JCT region and decreased outflow facility. Versican immunostaining was not completely eliminated in the versican-silenced TM, but complete abolishment was not expected, as versican mRNA is only knocked down and not completely eliminated. Moreover, endogenous versican that was already deposited in the ECM may not be turned over completely within the time frame of the perfusion experiment. Since versican binds many other ECM molecules, including fibronectin, CD44, fibrillins, and tenascins,[2] reduced versican levels likely disrupt TM ECM organization. Previous antisense studies have shown that depletion of versican increases tropoelastin mRNA levels, elastin deposition, and fiber formation in vascular smooth muscle cells.[26] Elastin assembly or other ECM component structures may therefore be altered in versican-depleted TMs. In the primary open-angle glaucoma (POAG) TM, there is a significant increase in the number of elastin-containing sheath-derived plaques in the JCT region.[55–59] In the present study, we show that versican stains in a fibrillar pattern that is perpendicular to Schlemm's canal in normal human eyes. This pattern is similar to pillars of elastic fibers containing fibrillins and microfibril associated protein (MFAP)-1/2 described recently.[60] We hypothesize that these pillars of staining may represent actual flow channels through the TM as this pattern of staining predominated in densely Qdot-labeled regions. The versican molecules with their attached CS GAG chains may be essential to distributing the load within these channels to maintain their openness and prevent collapse. In versican-silenced human TM, there is a reduction of versican molecules and hence GAG chains. The versican molecules that remain are therefore subject to a higher load, which could lead to compaction, narrowing, and/or collapse of the outflow channels. The results presented here support this hypothesis, as there was loss of the pillar pattern of versican immunostaining in the JCT of versican-silenced TMs and H&E staining revealed disorganization in the tissue. Hyaluronidase pretreatment of tissue sections reduced hematoxylin staining in the JCT of versican-silenced eyes, suggesting that HA contributed, at least in part, to the altered staining patterns observed. These macromolecular changes in tissue structure were coincident with a decrease in outflow facility. Together, these observations argue that versican is a central component of the outflow resistance and may function to guide the proper structural organization of HA and other ECM molecules to facilitate open flow channels in the TM.

Lentiviral knockdown of versican caused opposite effects on outflow in human and porcine eyes. Versican silencing decreased outflow in human eyes but increased outflow facility in porcine eyes under identical experimental conditions. The reason for these opposite effects remains unclear. Prior outflow facility experiments where GAGase enzymes were perfused into primate and nonprimate eyes also produced differential responses.[6,14,19,61–63] Nuanced variations in ECM structure or composition probably account for the observed reciprocal response in outflow facility shown here and the differential results between species in other studies. However, it is likely that, in all species, versican contributes to both physical outflow resistance and the three-dimensional structural organization of the ECM in the JCT region. Further studies are needed to accurately evaluate these differences in primate and nonprimate outflow resistance.

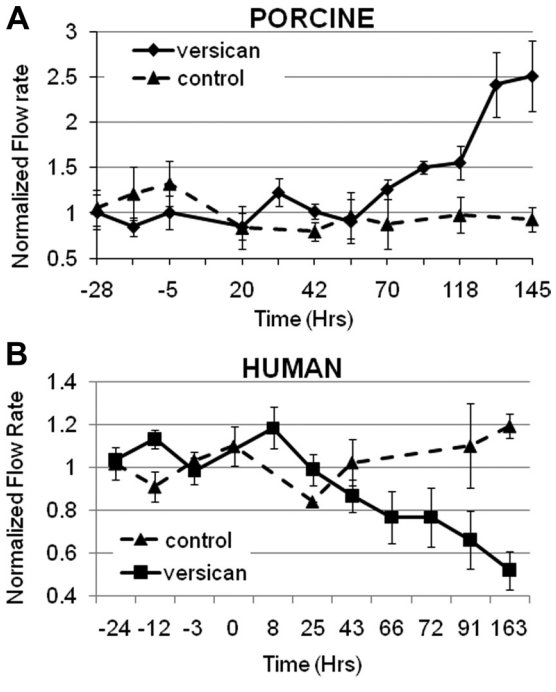

FIGURE 7. Effects of versican silencing on outflow facility. Perfused anterior segments were treated with control or versican shRNA lentivirus and outflow was monitored for several days. (**A**) Porcine anterior segments and (**B**) human anterior segments were stabilized in perfusion culture, and lentivirus was applied at time point 0. Values represent the mean ± SEM where $n = 5$ for versican-silenced eyes and $n = 4$ for control eyes. Flow rates were normalized based on pretreatment flow rates. Student's *t*-test comparing versican shRNA with control shRNA treatments gave $P = 0.05$ for porcine eyes and $P = 0.005$ for human eyes.

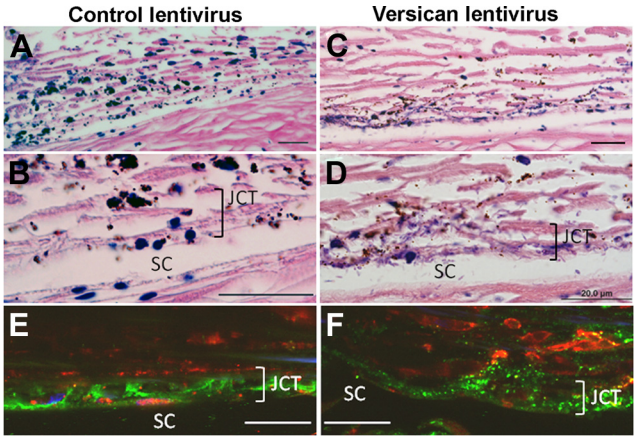

FIGURE 8. H&E histochemistry and versican immunostaining of human TM after infection with control lentivirus (**A**, **B**, **E**) and versican-silencing lentivirus (**C**, **D**, **F**). H&E staining showed that the JCT region was disorganized after versican silencing. (**E**, **F**) Immunofluorescence images show that pillars of versican immunostaining (*green*) were disrupted in the JCT region of versican-silenced TMs. CD44 (*red*) labels TM cells. The images in (**E**) and (**F**) were from an area of moderate Qdot labeling (also in *red*). Scale bars, 20 μm.

In areas of high Qdot labeling, reduced versican levels will also affect GAG chain concentration. Analysis of alternative splicing in areas of dense and sparse Qdot labeling showed that the V1 and V2 isoforms were relatively increased in areas of dense labeling, coincident with a reduction in total versican levels. By elimination, this suggests that V0, the longest versican splice variant, is more abundant in sparsely labeled areas. The V0 variant has 17 to 23 CS chains attached, whereas the V1 and V2 variants only have 12 to 15 and 5 to 8 CS attachment sites, respectively.[2] Therefore, in addition to reduced amounts of versican, areas with dense Qdot labeling may have a higher number of splice forms with fewer CS GAG chains. This suggests that CS GAG concentration is reduced in densely Qdot-labeled areas, which correlates with the increased outflow facility observed in ChGn-silenced eyes. Decreased CS concentrations caused by reduced versican would affect outflow resistance since the hydration capacity would be reduced, which in turn would lead to decreased resistance and increased aqueous humor passage through these areas. According to the same argument, in areas of sparse Qdot labeling, versican levels were increased and the versican V0 isoform, containing the largest number of CS chains, may be enriched. Of interest, in POAG eyes where outflow is reduced, CS chains were found to accumulate in the JCT region.[14,62] Changes in CS GAG chain concentration may also affect ECM protein–protein interactions, since chlorate, an inhibitor of GAG sulfation, induces atypical interactions between tenascin C and fibronectin.[19] Thus, regional alterations in versican levels, splice forms, or both will affect CS GAG chain concentration and may be a mechanism by which TM cells modify their ECM to homeostatically adjust outflow resistance.

Versican levels may also affect HA deposition into the ECM. Our previous study revealed variability in the staining pattern of HA-binding protein in human TM, which was suggestive of segmental flow.[19] Since versican assembles HA into aggregates,[26] a reduced amount of versican suggests that HA may also be depleted or disorganized in densely labeled areas. Conversely, in areas of sparse Qdot labeling, larger amounts of versican could assemble HA into aggregates, thereby increasing local HA concentration. A prior in vitro study showed that outflow decreased with increasing HA concentrations,[64] and intracameral application of HA to rat anterior chambers increased IOP.[65]

To further investigate the role of CS chains in outflow resistance, we silenced the ChGn gene, which is an enzyme unique to CS GAG chain biosynthesis. In perfusion culture, we found an increase in outflow facility in both human and porcine anterior segments. This result supports previous observations using a chemical modifier of GAG biosynthesis, β-xyloside, or by enzymatic digestion of CS chains with chondroitinase ABC in porcine, bovine, and Cynomolgus monkey eyes.[10,16,19,66] Thus, a reduction of CS chains increases outflow facility in both human and porcine eyes. This observation correlates with reduced levels of versican in areas of dense Qdot labeling and with the contrary observations that increased CS concentrations are detected in POAG TM and intracameral administration of CS to the anterior chamber in rats causes IOP to increase.[14,62,67]

In summary, segmental distribution of versican suggests that it is a central component of the outflow resistance and may be required to organize GAGs and other ECM components to facilitate open flow channels in the TM. This study represents a first step in identifying the molecular composition of outflow resistance and how specific ECM components can be manipulated to alter outflow facility.

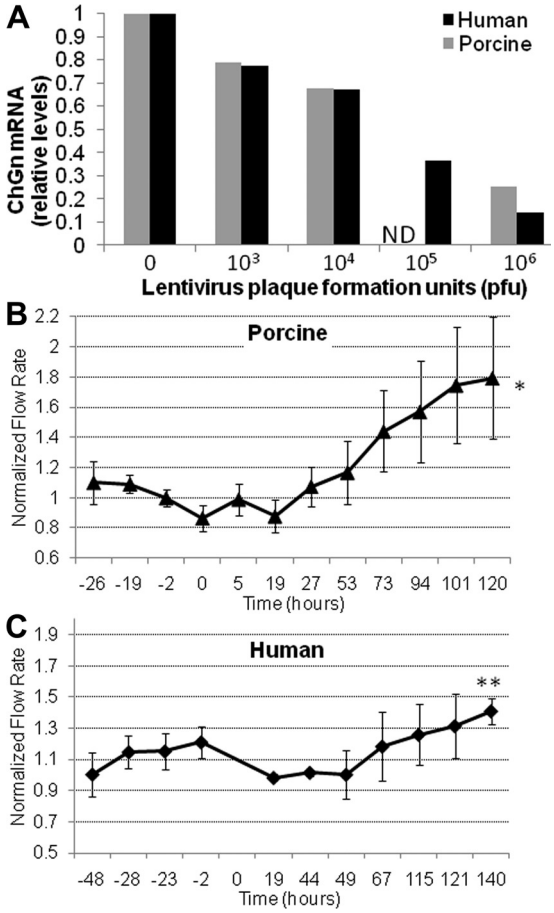

FIGURE 9. Effect of ChGn silencing on outflow. (**A**) Dilutions of ChGn shRNA lentivirus were added to human and porcine TM cell cultures and ChGn silencing efficacy evaluated by qRT-PCR 48 hours after infection. Values represent the change ratio relative to mock-infected TM cells. (**B**) Porcine and (**C**) human anterior segments were perfused with ChGn shRNA lentivirus at time 0, and effects on flow rate were assessed. Values represent the mean ± SEM; $n = 4$ for porcine and $n = 5$ for human. Significance determined by Student's *t*-test; $^{*}P = 0.03$, $^{**}P = 0.04$.

Acknowledgments

The authors thank Ruth Phinney (Oregon Lions Eye Bank) for coordinating human eye procurement, Carolyn Gendron for tissue sectioning, and Genevieve Long, PhD, for editorial assistance.

References

1. Johnson M. What controls aqueous humour outflow resistance?. *Exp Eye Res.* 2006;82:545–557.
2. Acott TS, Kelley MJ. Extracellular matrix in the trabecular meshwork (review). *Exp Eye Res.* 2008;86:543–561.
3. Ethier CR. The inner wall of Schlemm's canal. *Exp Eye Res.* 2002; 74:161–172.
4. Maepea O, Bill A. Pressures in the juxtacanalicular tissue and Schlemm's canal in monkeys. *Exp Eye Res.* 1992;54:879–883.
5. Bárány EH, Woodin AM. Hyaluronic acid and hyaluronidase in the aqueous humour and the angle of the anterior chamber. *Acta Physiol Scand.* 1954;33:257–290.
6. Francois J. The importance of the mucopolysaccharides in intraocular pressure regulation. *Invest Ophthalmol.* 1975;14:173–176.
7. Rohen JW, Lütjen-Drecoll E. *Biology of the Trabecular Meshwork.* Stuttgart: F.K. Schattauer, Verlap; 1982:141–166.
8. Hernandez MR, Gong H. *Extracellular Matrix of the Trabecular Meshwork and Optic Nerve Head.* 2nd ed. St. Louis: Mosby-Year Book, Inc.; 1996:213–250.
9. Yue BYJT. The extracellular matrix and its modulation in the trabecular meshwork. *Surv Ophthalmol.* 1996;40:379–390.
10. Lütjen-Drecoll E. Functional morphology of the trabecular meshwork in primate eyes. *Prog Retin Eye Res.* 1999;18:91–119.
11. Overby DR, Stamer WD, Johnson M. The changing paradigm of outflow resistance generation: towards synergistic models of the JCT and inner wall endothelium. *Exp Eye Res.* 2009;88:656–670.
12. Knepper PA, Breen M, Weinstein HG, Blacik LJ. Intraocular pressure and glycosaminoglycan distribution in the rabbit eye: effect of age and dexamethasone. *Exp Eye Res.* 1978;27:567–575.
13. Knepper PA, Farbman AI, Telser AG. Exogenous hyaluronidases and degradation of hyaluronic acid in the rabbit eye. *Invest Ophthalmol Vis Sci.* 1984;25:286–293.
14. Knepper PA, Goossens W, Palmberg PF. Glycosaminoglycan stratification of the juxtacanalicular tissue in normal and primary open-angle glaucoma. *Invest Ophthalmol Vis Sci.* 1996;37:2414–2425.
15. Hubbard W, Johnson M, Gong H, et al. Intraocular pressure and outflow facility are unchanged following acute and chronic intracameral chondroitinase ABC and hyaluronidase in monkeys. *Exp Eye Res.* 1997;65:177–190.
16. Sawaguchi S, Yue B, Yeh P, Tso M. Effects of intracameral injection of chondroitinase ABC in vivo. *Arch Ophthalmol.* 1992;110:110–117.
17. Keller K, Aga M, Bradley J, Kelley M, Acott T. Extracellular matrix turnover and outflow resistance. *Exp Eye Res.* 2009;88:676–682.
18. Keller K, Bradley JM, Acott TS. Differential effects of ADAMTSs −1, −4, and −5 in the trabecular meshwork. *Invest Ophthalmol Vis Sci.* 2009;50:5769–5777.
19. Keller KE, Bradley JM, Kelley MJ, Acott TS. Effects of modifiers of glycosaminoglycan biosynthesis on outflow facility in perfusion culture. *Invest Ophthalmol Vis Sci.* 2008;49:2495–2505.
20. Bradley JMB, Kelley MJ, Zhu XH, Anderssohn AM, Alexander JP, Acott TS. Effects of mechanical stretching on trabecular matrix metalloproteinases. *Invest Ophthalmol Vis Sci.* 2001;42:1505–1513.
21. Bradley JMB, Vranka JA, Colvis CM, et al. Effects of matrix metalloproteinase activity on outflow in perfused human organ culture. *Invest Ophthalmol Vis Sci.* 1998;39:2649–2658.
22. Fautsch MP, Johnson DH. Aqueous humor outflow: what do we know?—where will it lead us? *Invest Ophthalmol Vis Sci.* 2006; 47:4181–4187.
23. Wirtz MK, Bradley JMB, Demories J, et al. Proteoglycan expression by human trabecular meshworks. *Curr Eye Res.* 1997;16:412–421.
24. Wight TN. Versican: a versatile extracellular matrix proteoglycan in cell biology. *Curr Opin Cell Biol.* 2002;14:617–623.
25. Scott JE. Elasticity in extracellular matrix 'shape modules' of tendon, cartilage, etc. a sliding proteoglycan-filament model. *J Physiol.* 2003; 553:335–343.
26. Huang R, Merrilees MJ, Braun K, et al. Inhibition of versican synthesis by antisense alters smooth muscle cell phenotype and induces elastic fiber formation in vitro and in neointima after vessel injury. *Circ Res.* 2006;98:370–377.
27. LeBaron RG, Zimmermann DR, Ruoslahti E. Hyaluronate binding properties of versican. *J Biol Chem.* 1992;267:10003–10010.
28. Bradley JM, Kelley MJ, Rose A, Acott TS. Signaling pathways used in trabecular matrix metalloproteinase response to mechanical stretch. *Invest Ophthalmol Vis Sci.* 2003;44:5174–5181.
29. Keller KE, Kelley MJ, Acott TS. Extracellular matrix gene alternative splicing by trabecular meshwork cells in response to mechanical stretching. *Invest Ophthalmol Vis Sci.* 2007;48:1164–1172.
30. Gottanka J, Chan D, Eichhorn M, Lütjen-Drecoll E, Ethier CR. Effects of TGF-beta2 in perfused human eyes. *Invest Ophthalmol Vis Sci.* 2004;45:153–158.
31. Fleenor DL, Shepard AR, Hellberg PE, Jacobson N, Pang IH, Clark AF. TGFbeta2-induced changes in human trabecular meshwork: implications for intraocular pressure. *Invest Ophthalmol Vis Sci.* 2006;47:226–234.
32. Zhao X, Ramsey KE, Stephan DA, Russell P. Gene and protein expression changes in human trabecular meshwork cells treated with transforming growth factor-beta. *Invest Ophthalmol Vis Sci.* 2004;45:4023–4034.
33. Zhao X, Russell P. Versican splice variants in human trabecular meshwork and ciliary muscle. *Mol Vis.* 2005;11:603–608.
34. Hann CR, Bahler CK, Johnson DH. Cationic ferritin and segmental flow through the trabecular meshwork. *Invest Ophthalmol Vis Sci.* 2005;46:1–7.
35. Hann CR, Fautsch MP. Preferential fluid flow in the human trabecular meshwork near collector channels. *Invest Ophthalmol Vis Sci.* 2009;50:1692–1697.
36. Battista SA, Lu Z, Hofmann S, Freddo T, Overby DR, Gong H. Reduction of the available area for aqueous humor outflow and increase in meshwork herniations into collector channels following acute IOP elevation in bovine eyes. *Invest Ophthalmol Vis Sci.* 2008;49:5346–5352.
37. Lu Z, Overby DR, Scott PA, Freddo TF, Gong H. The mechanism of increasing outflow facility by rho-kinase inhibition with Y-27632 in bovine eyes. *Exp Eye Res.* 2008;86:271–281.
38. Buller C, Johnson D. Segmental variability of the trabecular meshwork in normal and glaucomatous eyes. *Invest Ophthalmol Vis Sci.* 1994;35:3841–3851.
39. de Kater AW, Melamed S, Epstein DL. Patterns of aqueous humor outflow in glaucomatous and nonglaucomatous human eyes: a tracer study using cationized ferritin. *Arch Ophthalmol.* 1989;107: 572–576.
40. Acott TS, Kingsley PD, Samples JR, Van Buskirk EM. Human trabecular meshwork organ culture: morphology and glycosaminoglycan synthesis. *Invest Ophthalmol Vis Sci.* 1988;29:90–100.
41. Parc C, Johnson D, Brilakis H. Giant vacuoles are found preferentially near collector channels. *Invest Ophthalmol Vis Sci.* 2000;41: 2984–2990.
42. Aga M, Bradley J, Keller K, Kelley M, Acott T. Specialized podosome- or invadopodia-like structures (PILS) for focal trabecular meshwork extracellular matrix turnover. *Invest Ophthalmol Vis Sci.* 2008;49:5353–5365.
43. Silbert JE, Sugumaran G. Biosynthesis of chondroitin/dermatan sulfate. *IUBMB Life.* 2002;54:177–186.
44. Uyama T, Kitagawa H, Tamura Ji J, Sugahara K. Molecular cloning and expression of human chondroitin N-acetylgalactosaminyltransferase: the key enzyme for chain initiation and elongation of chondroitin/dermatan sulfate on the protein linkage region tetrasaccharide shared by heparin/heparan sulfate. *J Biol Chem.* 2002;277:8841–8846.
45. Gotoh M, Sato T, Akashima T, et al. Enzymatic synthesis of chondroitin with a novel chondroitin sulfate N-acetylgalactosaminyltransferase that transfers N-acetylgalactosamine to glucuronic acid in initiation and elongation of chondroitin sulfate synthesis. *J Biol Chem.* 2002;277:38189–38196.

46. Loewen N, Fautsch MP, Peretz M, et al. Genetic modification of human trabecular meshwork with lentiviral vectors. *Hum Gene Ther.* 2001;12:2109–2119.
47. Khare PD, Loewen N, Teo W, et al. Durable, safe, multi-gene lentiviral vector expression in feline trabecular meshwork. *Mol Ther.* 2008;16:97–106.
48. Uyama T, Kitagawa H, Tanaka J, Tamura J, Ogawa T, Sugahara K. Molecular cloning and expression of a second chondroitin N-acetylgalactosaminyltransferase involved in the initiation and elongation of chondroitin/dermatan sulfate. *J Biol Chem.* 2003;278:3072–3078.
49. Sakai K, Kimata K, Sato T, et al. Chondroitin sulfate N-acetylgalactosaminyltransferase-1 plays a critical role in chondroitin sulfate synthesis in cartilage. *J Biol Chem.* 2007;282:4152–4161.
50. Ethier CR, Chan D-H. Cationic ferritin changes outflow facility in human eyes whereas anionic ferritin does not. *Invest Ophthalmol Vis Sci.* 2001;42:1795–1802.
51. Inomata H, Bill A, Smelser GK. Aqueous humor pathways through the trabecular meshwork and into Schlemm's canal in the cynomolgus monkey (Macaca irus): an electron microscopic study. *Am J Ophthalmol.* 1972;73:760.
52. Grande-Allen KJ, Calabro A, Gupta V, Wight TN, Hascall VC, Vesely I. Glycosaminoglycans and proteoglycans in normal mitral valve leaflets and chordae: association with regions of tensile and compressive loading. *Glycobiology.* 2004;14:621–633.
53. Tumminia SJ, Mitton KP, Arora J, Zelenka P, Epstein PL, Russell P. Mechanical stretch alters the actin cytoskeletal network and signal transduction in human trabecular meshwork cells. *Invest Ophthalmol Vis Sci.* 1998;39:1361–1371.
54. Vittal V, Rose A, Gregory KE, Kelley MJ, Acott TS. Changes in gene expression by trabecular meshwork cells in response to mechanical stretching. *Invest Ophthalmol Vis Sci.* 2005;46:2857–2868.
55. Alvarado J, Murphy C, Juster R. Trabecular meshwork cellularity in primary open-angle glaucoma and nonglaucomatous normals. *Ophthalmology.* 1984;91:564–579.
56. Tektas OY, Lütjen-Drecoll E. Structural changes of the trabecular meshwork in different kinds of glaucoma. *Exp Eye Res.* 2009;88:769–775.
57. Ueda J, Wentz-Hunter K, Yue BY. Distribution of myocilin and extracellular matrix components in the juxtacanalicular tissue of human eyes. *Invest Ophthalmol Vis Sci.* 2002;43:1068–1076.
58. Lütjen-Drecoll E, Shimizu T, Rohrbach M, Rohen JW. Quantitative analysis of "plaque material" in the inner- and outer wall of Schlemm's canal in normal and glaucomatous eyes. *Exp Eye Res.* 1986;42:443–455.
59. Lütjen-Drecoll E, Futa R, Rohen JW. Ultrahistochemical studies on tangential sections of the trabecular meshwork in normal and glaucomatous eyes. *Invest Ophthalmol Vis Sci.* 1981;21:563–573.
60. Hann CR, Fautsch MP. The elastin fiber system between and adjacent to collector channels in the human juxtacanalicular tissue. *Invest Ophthalmol Vis Sci.* 2011;52:45–50.
61. Gong H, Freddo TF, Johnson M. Age-related changes of sulfated proteoglycans in the normal human trabecular meshwork. *Exp Eye Res.* 1992;55:691–709.
62. Knepper PA, Goossens W, Hvizd M, Palmberg PF. Glycosaminoglycans of the human trabecular meshwork in primary open-angle glaucoma. *Invest Ophthalmol Vis Sci.* 1996;37:1360–1367.
63. Tawara A, Varner HH, Hollyfield JG. Distribution and characterization of sulfated proteoglycans in the human trabecular tissue. *Invest Ophthalmol Vis Sci.* 1989;30:2215–2231.
64. Knepper PA, Fadel JR, Miller AM, et al. Reconstitution of trabecular meshwork GAGs: influence of hyaluronic acid and chondroitin sulfate on flow rates. *J Glaucoma.* 2005;14:230–238.
65. Benozzi J, Nahum LP, Campanelli JL, Rosenstein RE. Effect of hyaluronic acid on intraocular pressure in rats. *Invest Ophthalmol Vis Sci.* 2002;43:2196–2200.
66. Sawaguchi S, Lam TT, Yue BYJT, Tso MOM. Effects of glycosaminoglycan-degrading enzymes on bovine trabecular meshwork in organ culture. *J Glaucoma.* 1993;2:80–86.
67. Belforte N, Sande PH, de Zavalia N, Knepper PA, Rosenstein RE. Effect of chondroitin sulfate on intraocular pressure in rats. *Invest Ophthalmol Vis Sci.* 2010;51:5768–5775.